



# A First-principles study of the O, O<sub>2</sub>, OH, and HO<sub>2</sub> adsorption on the Fe (100) surface

Muhamad Akrom

Department of Informatics Engineering, Faculty of Computer Science, Dian Nuswantoro University,  
Semarang 50131, Indonesia  
email: [akrom5787@gmail.com](mailto:akrom5787@gmail.com)

## ARTICLE INFO

### Article History:

Received : 11-09-2021  
Revised : 17-11-2021  
Accepted : 18-11-2021  
Online : 18-11-2021

### Keywords:

DFT  
Adsorption  
Iron surface

## ABSTRACT

**Abstract:** The purpose of this study was to investigate the interaction between O, O<sub>2</sub>, OH, and HO<sub>2</sub> species on the Fe(100) surface using the DFT method. The DFT calculation provides specific information of the electronic structure of a molecules in ground state. The results show that the O atom preferred to be adsorbed on the hollow site, the OH species was adsorbed on the bridge site, while the O<sub>2</sub> molecule was dissociated into two O atoms where both were adsorbed on the hollow site. Furthermore, when the H atom is attached to one of the O atoms of the dissociated O<sub>2</sub> molecule, the OH species is formed which is adsorbed at the bridge site, and another O atom which remains adsorbed at the hollow site. This study can provide preliminary information on the adsorption mechanism of O, O<sub>2</sub>, OH, and HO<sub>2</sub> species in explaining the electrochemical corrosion mechanism in our next work.



**Abstrak:** Penelitian ini bertujuan untuk mengetahui interaksi antara spesi O, O<sub>2</sub>, OH, dan HO<sub>2</sub> pada permukaan Fe(100) menggunakan metode DFT. Perhitungan DFT memberikan informasi spesifik tentang struktur elektronik molekul dalam keadaan dasar. Hasil penelitian menunjukkan bahwa atom O lebih suka teradsorpsi pada situs berongga, spesi OH teradsorpsi pada situs jembatan, sedangkan molekul O<sub>2</sub> terdisosiasi menjadi dua atom O dimana keduanya teradsorpsi pada situs berongga. Selanjutnya, ketika atom H terikat pada salah satu atom O dari molekul O<sub>2</sub> terdisosiasi, terbentuk spesies OH yang teradsorpsi di situs jembatan, dan atom O lain yang tetap teradsorpsi di situs berongga. Penelitian ini dapat memberikan informasi awal tentang mekanisme adsorpsi spesi O, O<sub>2</sub>, OH, dan HO<sub>2</sub> dalam menjelaskan mekanisme korosi elektrokimia pada penelitian kami selanjutnya.



<https://doi.org/10.31764/justek.vXiY.ZZZ>



This is an open access article under the [CC-BY-SA](https://creativecommons.org/licenses/by-sa/4.0/) license

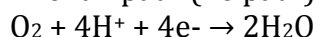
## A. INTRODUCTION

The phenomenon of corrosion in materials is a very important concern for industrial and academic because corrosion causes enormous losses. Corrosion loss in the United States per year is estimated at 3.1% of gross domestic product (GDP) or about 364 billion dollars (Rapp, 2006). Corrosion is a process of degrading material due to electrochemical reactions with corrosive environments (Trethewey, 1988). If there is a transfer of electrons from the anode to the cathode, a corrosion event occurs. The corrosion reaction is an electrochemical reaction that consists of an oxidation reaction at the anode and a reduction reaction at the cathode. The rate of electrons generated in the oxidation

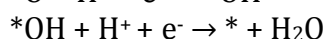
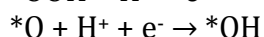
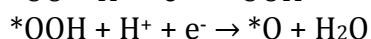
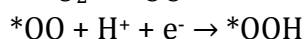
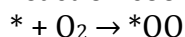
reaction corresponds to the rate at which electrons are consumed by the reduction reaction.

In the event of corrosion generally, the reaction that occurs in the cathode is oxygen reduction reaction (ORR). ORR can take place through two pathways, namely the partial path (2 electrons) and the full path (4 electrons). The partial path involves the production of adsorbed hydrogen peroxide ( $H_2O_2$ ) whereas the full path is more efficient because it does not involve the production of hydrogen peroxide (Stacy et al., 2017; Reda et al., 2018; Safakas et al., 2019). In an acidic environment, ORR can take place in two ways, namely the full path and the partial path.

The full path (4e path):

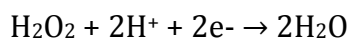
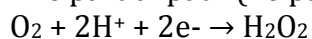


The full path is a path that generally occurs on plain metal surfaces (Ng et al., 2020). The reaction coordinates for the full path in an acidic environment are as follows:



where  $*OO$ ,  $*OOH$ ,  $*O$ , and  $*OH$  are chemical species adsorbed on the metal surface.

The partial path (2e path):



Investigations on the surface of iron are fundamental to increasing early understanding of the interactions between ferrous metals and chemical species. Several experimental and theoretical studies on the chemical species adsorption on Fe surfaces have been carried out in recent decades. The adsorption of the species ( $O$ ,  $O_2$ ,  $OH$ , and  $HO_2$ ) on the Fe surface is very important to understand in explaining the electrochemical corrosion mechanism. Until now, the interaction of  $O$ ,  $O_2$ ,  $OH$ , and  $HO_2$  species on the iron surface is still an extensive experimental and theoretical study. Early studies on the interaction of the  $O$  atom with the Fe (100) surface experimentally (Sakisaka et al., 1984) and theoretically (Blonski et al., 2005; Cao et al., 2010) show that more stable oxygen atoms are adsorbed at hollow sites. The interaction of the  $O_2$  molecule on the Fe (100) surface experimentally (Lu et al., 1989) and theoretically (Blonski et al., 2008; Chen et al., 2020) showed that there was irregular dissociative adsorption. The theoretical investigation of the  $OH$  species adsorbed on the Fe (100) surface showed that the bridge site is the preferred adsorption site (Wang et al., 2016; Chen et al., 2020) as confirmed in experimental studies (Anderson et al., 1981).

This study aims to gain a more effective understanding of the adsorption process of species ( $O$ ,  $O_2$ ,  $OH$ , and  $HO_2$ ) on the Fe(100) surface, therefore we present a systematic first-principle study based on electronic and energetic properties.

## B. RESEARCH METHODS

All calculations were performed by using the Quantum Espresso software package (Giannozzi et al., 2017; Kokalj et al., 2020). The interaction between electrons and atomic nuclei is described by the ultrasoft pseudopotential method with the cutoff energy of 40 Ry and the cutoff energy of 200 Ry was employed for plane wave expansions (Vanderbilt et al., 1990). We adopt the generalized gradient approximation (GGA) within the Perdew-Burke-Ernzerhof (PBE) for exchange-correlation energy (Perdew et al., 1996). To ensure

the energy accuracy of the system, we applied the force convergence criterion is 0.0015 eV/Å, and the self-consistent field convergence criterion of 0.0027 meV. We use spin-polarization to accurately describe the magnetism of the system. The Broyden-Fletcher Goldfarb-Shanno (BFGS) method is used for structure optimization under periodic boundary conditions (Fischer et al., 1992). To prevent the interaction between periodic images, a vacuum layer of 15 Å was applied. We use  $2 \times 2 \times 1$  k-point Monkhorst-Pack to perform calculation in our system.

Moreover, the adsorption energy is also calculated to analyze the stability of the molecules after adsorption. The adsorption energy ( $E_{\text{ads}}$ ) is calculated in Eq. 1. The more negative the  $E_{\text{ads}}$  value indicates the most stable adsorption.

$$E_{\text{ads}} = E_{\text{surface/molecule}} - E_{\text{surface}} - E_{\text{molecule}}$$

where  $E_{\text{surface/molecule}}$  and  $E_{\text{surface}}$  is the energy of the surface after and before adsorption of the molecule, and  $E_{\text{molecule}}$  is the energy of the isolated molecule.

The surface structure of Fe (100) is modeled with a supercell approach with periodic boundary conditions. We calculate the lattice parameter of bulk Fe with bcc symmetry to ensure that our calculations are valid. Our calculations (2.85 Å) are consistent with the previous calculations (2.82 Å) (Yang et al., 2019) and experimental results (2.87 Å) (Kohlhaas et al., 1967). The Monkhorst-Pack k-point grid is  $12 \times 12 \times 12$  which is used as the equilibrium lattice parameter for the bulk Fe calculations (Mohnkorst et al., 1976). The surface structure of Fe is built based on the optimized bulk Fe. The slabs consist of 4 layers and  $3 \times 3$  supercells are applied to estimate the properties of O, OH, O<sub>2</sub>, and HO<sub>2</sub> species dissociative adsorption on the Fe (100) surface. The atoms in the top two layers are relaxed while the atoms in the other layers are fixed. The isolated species (O, OH, O<sub>2</sub>, and HO<sub>2</sub>) are modeled in  $30 \times 30 \times 30$  Å<sup>3</sup> supercells and used a gamma k-point. The possible adsorption sites and structural model of the Fe (100) surface are shown in Fig. 1.

The adsorption energy of O, OH, and O<sub>2</sub> species on the Fe (100) surface was calculated based on common adsorption sites (i.e., bridge, hollow, and top) (Chew et al., 2018; Chen et al. 2020) as shown in Fig. 1a. Fig. 2, Fig. 3, and Fig. 4 display the top and side views of the initial position configuration before adsorbed on the Fe (100) surface of O, OH, and O<sub>2</sub>, respectively.

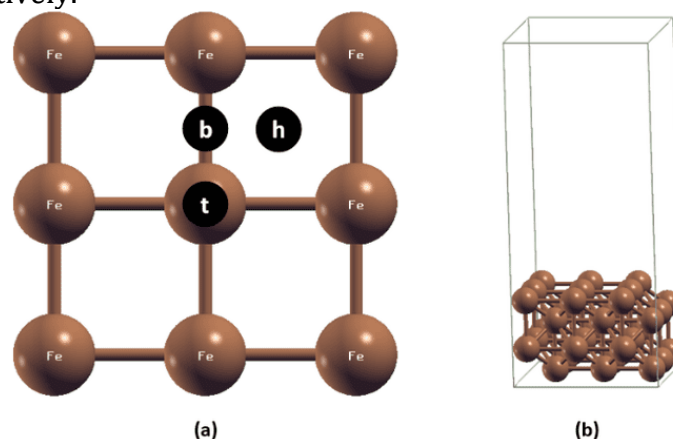


Fig. 1. (a) adsorption sites (bridge, hollow, and top) and (b) model of the Fe (100) surface.

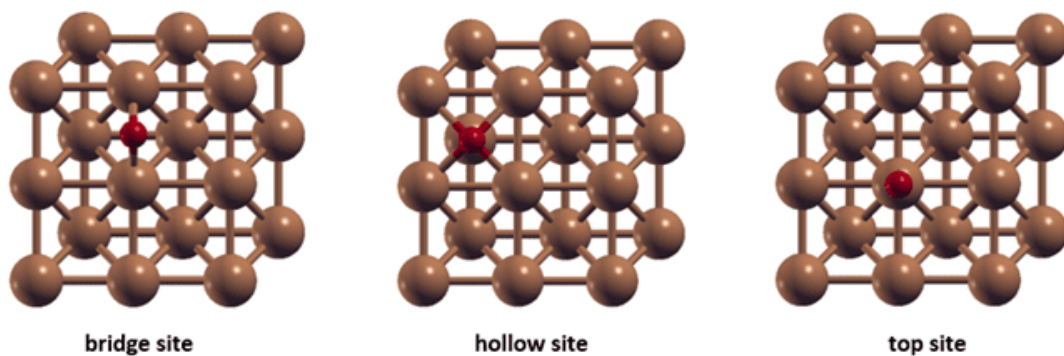


Fig. 2. Initial position of the O atom before adsorbed on the Fe (100) surface. Brown and red are colors of Fe and O atoms, respectively.

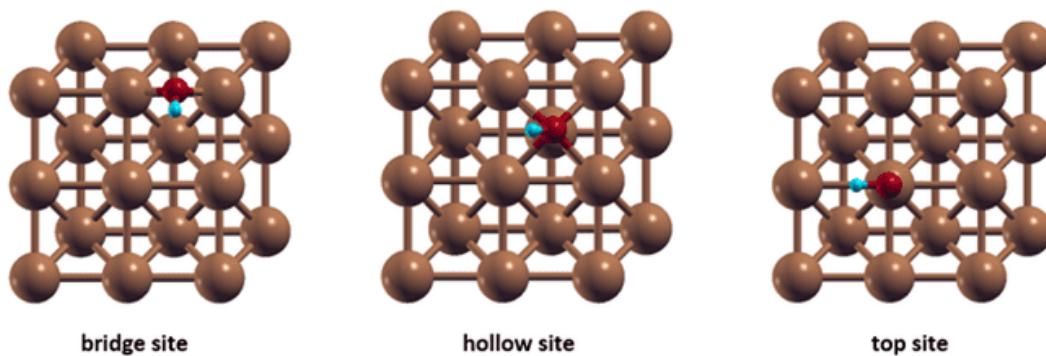


Fig. 3. Initial position of the OH species before adsorbed on the Fe (100) surface. Brown, red, and blue are atomic colors of Fe, O, and H atoms, respectively.

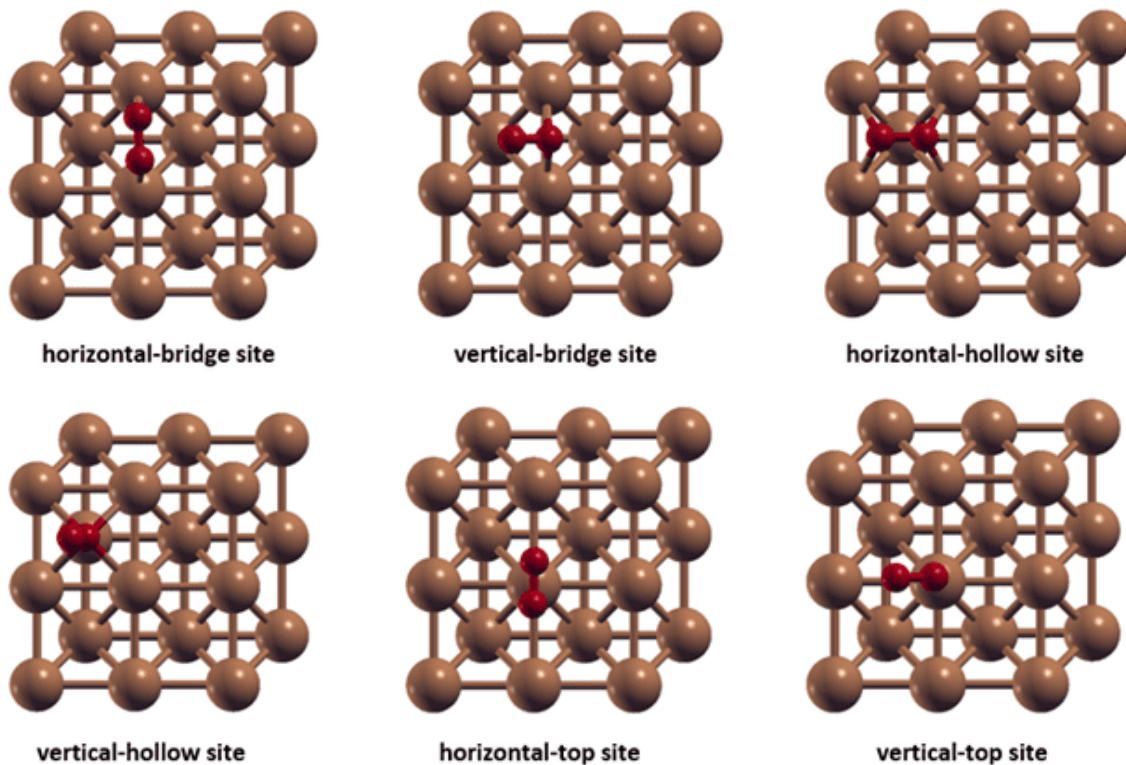


Fig. 4. Top and side views of the initial position of the O<sub>2</sub> molecule before adsorbed on the Fe (100) surface. Brown and red are atomic colors of Fe and O atoms, respectively.

## C. RESULT AND DISCUSSIONS

### 1. O adsorption on Fe (100) surface

In the present study, the adsorption energy of the O atom on the Fe (100) surface are evaluated in three different sites (bridge, hollow, and top) as shown in Fig. 2. The optimal geometry of each structure is shown in Figure 5. The adsorption energy and the distances between the atomic bonds are shown in Table 1 and Table 2, respectively. Based on Table 1, the adsorption energy values of the O atom on the bridge, hollow, and top sites are -3.06 eV, -3.53 eV, and -2.29 eV, respectively. All these adsorption energies are negative and large, this shows that the O atom can easily adsorb on the Fe (100) surface. The adsorption energy at the hollow site is the lowest, it shows that the hollow site is more favorable for adsorption, this result is in agreement with experiment (Cao et al., 2010) and theoretical calculation (Sakisaka et al., 1984).

Table 1. The adsorption energy of the O atom on the Fe (100) surface.

Site	Eads (eV)
B	-3.06
H	-3.53
T	-2.29

Table 2. The distance between O with nearest Fe.

Site	Bond	d (Å)
B	O-Fe1	1.22
	O-Fe2	1.27
H	O-Fe1	0.63
	O-Fe2	0.63
	O-Fe3	0.63
	O-Fe4	0.63
	O-Fe5	2.19
T	O-Fe1	1.63

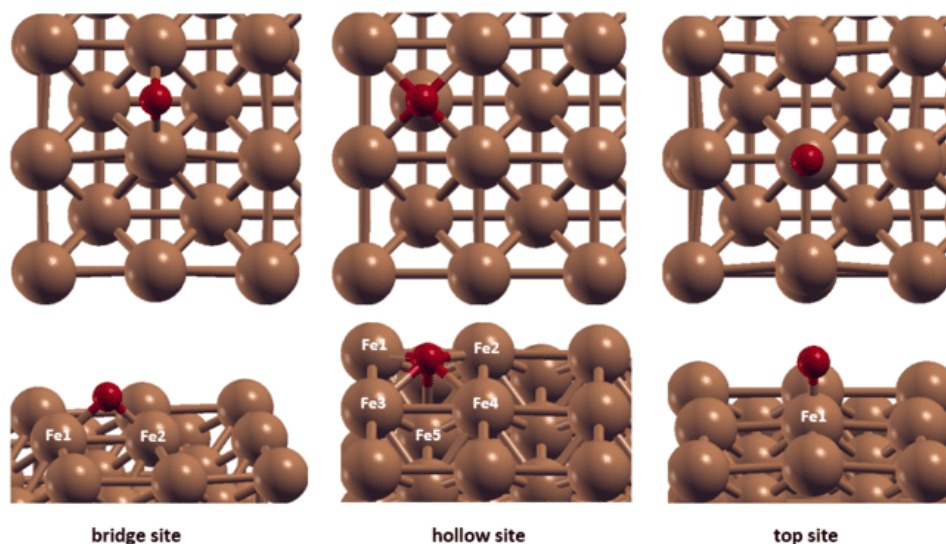


Fig. 5. Top and side views of the optimized position of the O atom after adsorbed on the Fe (100) surface. Brown and red are atomic colors of Fe and O atoms, respectively.



Seen in Fig. 5 that the O atom adsorbed on the Fe (100) surface binds with two nearest Fe atoms at the bridge site, while at the hollow and top sites it binds with five and one nearest Fe atoms, respectively. This shows that the atomic bonds at the hollow site are stronger than the other sites. This is also confirmed by the bond length between the O atom and the nearest Fe atom as can be seen in Table 2, where the bond distance at the hollow site is the shortest.

## 2. OH adsorption on Fe (100) surface

The adsorption energies of the OH species on the Fe (100) surface in three different sites (bridge, hollow, and top) as shown in Fig. 3 were calculated. The optimal geometry of each structure is shown in Figure 6. The adsorption energies and the distances between the atomic bonds are shown in Table 3 and Table 4, respectively. Based on Table 3, the adsorption energy value of the OH species at the bridge, hollow, and top sites are -4.34 eV, -4.17 eV, and -3.90 eV, respectively. All these adsorption energies are negative and large, this shows that the OH species can be easily adsorbed on the Fe (100) surface. The adsorption energy at the bridge site is the lowest, it shows that the bridge site is the most stable adsorption site, this result is consistent with experiment (Anderson et al., 1981) and theoretical study (Wang et al., 2018).

Based on Fig. 6, the OH species adsorbed on the Fe (100) surface binds with three nearest Fe atoms at the bridge site, while at the hollow and top sites it binds with two and one nearest Fe atoms, respectively. Moreover, the hollow site is an unstable adsorption site. From Table 4, the O-Fe bond length of the OH species with the nearest Fe atom is the longest compared to the other sites.

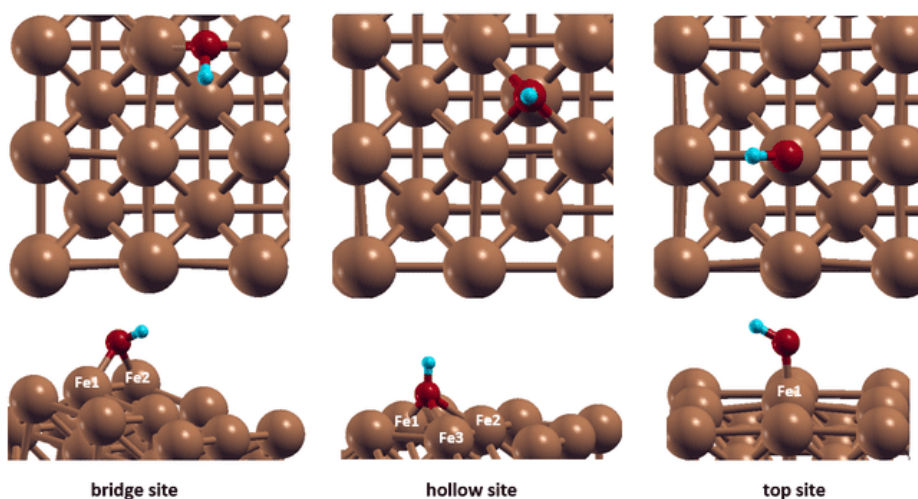


Fig. 6. Top and side views of the optimized position of the OH species after adsorbed on the Fe (100) surface. Brown, red, and blue are atomic colors of Fe, O, and H atoms, respectively.

Table 3. The adsorption energy of the OH species on the Fe (100) surface.

Site	Eads (eV)
B	-3.06
H	-3.53
T	-2.29

Table 4. The distance between the O atom of the OH species with the nearest Fe atom.

Site	Bond	d (Å)
B	O-Fe1	1.50
	O-Fe2	1.44
H	O-Fe1	1.22
	O-Fe2	0.21
	O-Fe3	0.22
T	O-Fe1	1.81

### 3. O<sub>2</sub> adsorption on Fe (100) surface

The adsorption energies of the O<sub>2</sub> molecule on the Fe (100) surface are calculated in three different sites (bridge, hollow, and top) with horizontal and vertical configuration as shown in Fig. 4. The optimal geometry of each structure is shown in Figure 5. The adsorption energies and the distances between the atomic bonds are shown in Table 5 and Table 6, respectively. From Table 5, the adsorption energies of the O<sub>2</sub> molecule on the horizontal-bridge, horizontal-hollow, and horizontal-top sites are -5.70 eV, -6.99 eV, and -6.47 eV, respectively, and the adsorption energies on the vertical-bridge, vertical-hollow, and vertical-top sites are -6.99 eV, -6.99 eV, and -2.64 eV, respectively. All these adsorption energies are negative and large, this shows that the O<sub>2</sub> molecule can be adsorbed on the Fe (100) surface easily.

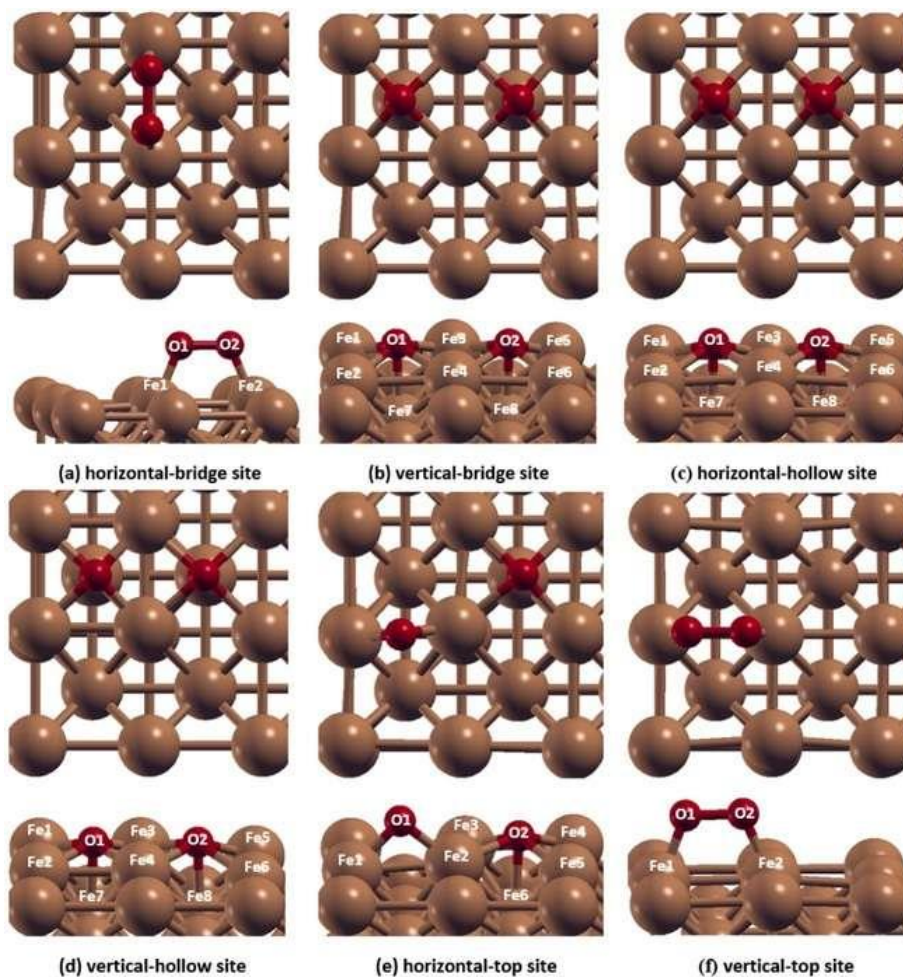


Fig. 7. Top and side views of the optimized position of the O<sub>2</sub> after adsorbed on the Fe (100) surface. Brown and red are atomic colors of Fe and O atoms, respectively.

The adsorption configuration of the O<sub>2</sub> molecule on the Fe (100) surface is irregular dissociative adsorption as shown in Fig. 7. From Fig. 7, the hollow site configuration (Fig. 7b, 7c, and 7d) is the most favorable dissociative adsorption site with the lowest adsorption energy. This result is in agreement with experiment (Lu et al. 1989) and theoretical calculation (Blonski et al., 2008; Chen et al., 2020). From Figures 7b, 7c, and 7d it is known that the O<sub>2</sub> molecule dissociates into two O atoms each interacting with the five nearest atoms of the Fe (100) surface with the bond distance between the O atom and the nearest Fe atom is the shortest as can be seen in Table 6. This shows that the hollow site is stronger than the other site configuration.

Table 5. The adsorption energy of the O<sub>2</sub> molecule on the Fe (100) surface.

	Site	Eads (eV)
Horizontal	B	-5.70
	H	-6.99
	T	-6.47
Vertical	B	-6.99
	H	-6.99
	T	-2.64

Table 6. The distance between the O atom of the O<sub>2</sub> species with the nearest Fe atom.

Site	Bond	d (Å)	Site	Bond	d (Å)
Horizontal	B	O1-Fe1	B	O1-Fe1	0.64
		O2-Fe2		O1-Fe2	0.64
		O1-Fe1		O1-Fe3	0.55
		O1-Fe2		O1-Fe4	0.55
		O1-Fe3		O1-Fe7	2.16
		O1-Fe4		O2-Fe3	0.55
	H	O1-Fe7	H	O1-Fe4	0.55
		O2-Fe3		O2-Fe5	0.64
		O2-Fe4		O2-Fe6	0.64
		O2-Fe5		O2-Fe8	2.16
		O2-Fe6		O1-Fe1	0.46
		O2-Fe8		O1-Fe2	0.47
Vertical	H	O1-Fe1	H	O1-Fe3	0.45
		O1-Fe2		O1-Fe4	0.46
		O2-Fe2		O1-Fe7	2.17
		O2-Fe3		O2-Fe3	0.45
		O2-Fe4		O1-Fe4	0.46
		O2-Fe5		O2-Fe5	0.69
	T	T	O2-Fe6	O2-Fe6	0.69
			O2-Fe8	O2-Fe8	2.17
			O1-Fe1	O1-Fe1	1.69
			O2-Fe2	O2-Fe2	1.67



#### 4. HO<sub>2</sub> adsorption on Fe (100) surface

The initial position of the HO<sub>2</sub> species adsorption site is to adjust to the most stable adsorption site of the O<sub>2</sub> molecule as shown in Figure 8a. Initially, one H atom is attached to one of the O atoms of the dissociated O<sub>2</sub> molecule. Fig. 8b, illustrates the results of the HO<sub>2</sub> adsorption which shows that H and O atoms formed OH bonds at the bridge site which is a stable site for OH as Fig. 6, besides that the other O atoms remain in the hollow site which is the stable site of the O atom as shown in Fig. 5. The adsorption energy of the HO<sub>2</sub> molecules is -7.15 eV, this adsorption energy has a negative and large, which indicates that the HO<sub>2</sub> molecule can be adsorbed on the surface of Fe (100) easily.

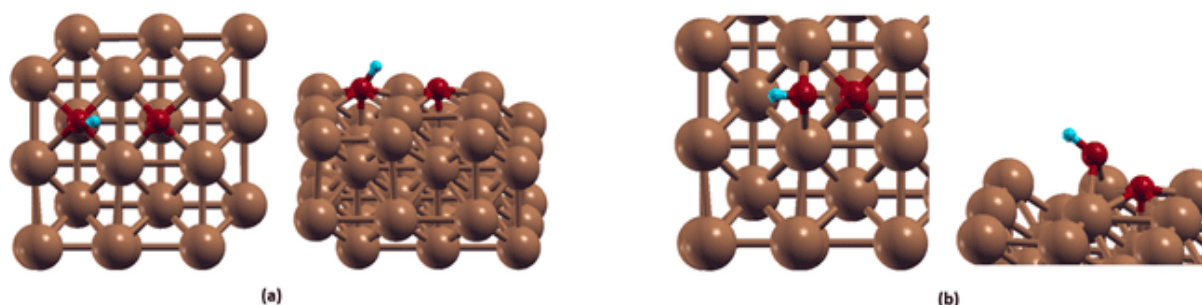


Fig. 8. Top and side views of the optimized position of HO<sub>2</sub> (a) before and (b) after adsorbed on Fe (100) surface. Brown, red, and blue are atomic colors of Fe, O and H, respectively.

#### D. CONCLUSIONS

In this study, the adsorption site configurations of O, O<sub>2</sub>, OH, and HO<sub>2</sub> species on the Fe (100) surface were investigated by DFT. The adsorption properties were analyzed by the adsorption energy and bond strength. It was found that O prefers adsorbed on the hollow site, OH is adsorbed on the bridge site, while O<sub>2</sub> is dissociated into two O atoms where both are adsorbed on the hollow site. Furthermore, when one of the O atoms of the dissociated O<sub>2</sub> molecule is bonded to the H atom, an OH is formed which is adsorbed on the bridge site, and another O atom that remains adsorbed on the hollow site. A detailed understanding of the adsorption process of O, O<sub>2</sub>, OH, and HO<sub>2</sub> species on the Fe (100) surface is very important in explaining the electrochemical corrosion mechanism.

#### REFERENCES

- A.B. Anderson. (1981). Reactions and structures of water on clean and oxygen covered Pt (111) and Fe (100). *Surface Science*, 105 (1981) 159-176.
- A. Kokalj, H. Behzadi, R. Farahati. (2020). DFT study of aqueous-phase adsorption of cysteine and penicillamine on Fe (110): Role of bond-breaking upon adsorption. *Applied Surface Science*, 514:145896, <https://doi.org/10.1016/j.apsusc.2020.145896>
- A. Safakas, G. Bampos, S. Bebelis. (2019). Oxygen reduction reaction on La<sub>0.8</sub>Sr<sub>0.2</sub>CoxFe<sub>1-x</sub>O<sub>3-δ</sub> perovskite/carbon black electrocatalysts in alkaline medium. *Applied Catalysis B: Environmental*, 244:225–232, <https://doi.org/10.1016/j.apcatb.2018.11.015>.
- B. Yang, K. Shi, H. Li, L. Jiang, C.H. Zhang. (2019). Water dissociative adsorption on the pre-covered Fe (100) surface from DFT computation. *Indian J Phys.*, 93 (8) : 1019–1029, <https://doi.org/10.1007/s12648-018-01372-9>.
- D. Vanderbilt. (1990). Soft self-consistent pseudopotentials in a generalized eigenvalue formalism. *Phys. Rev. B*, 41 : 7892–7895, <https://doi.org/10.1103/PhysRevB.41.7892>.
- H.J. Monkhorst & J.D. Pack. (1976). Special points for Brillouin-zone integrations. *Phys. Rev. B*, 13 : 5188.
- J.P. Lu, M.R. Albert, S.L. Bernasek. (1989). The adsorption of oxygen on Fe (100) surface. *Surface Science*. 215 (1989) 348-362.

- J.P. Perdew, K. Burke, M. Ernzerhof. (1996). Generalized gradient approximation made simple. *Phys. Rev. Lett.*, 77 (18) : 3865–3868, <https://doi.org/10.1103/PhysRevLett.77.3865>.
- J. Stacy, Y.N. Regmi, B. Leonard, M. Fan. (2017). The recent progress and future of oxygen reduction reaction catalysis: A review. *Renewable and Sustainable Energy Reviews*, 69 (2017) 401-414, <http://dx.doi.org/10.1016/j.rser.2016.09.135>.
- K.H. Chew, R. Kuwaharac, K. Ohno. (2018). First-principles study on the atomistic corrosion processes of iron. *Phys.Chem.Chem.Phys.*, 20:1653, DOI: 10.1039/c7cp04022a.
- M.F. Ng, D.J. Blackwood, H. Jin, T.L. Tan. (2020). DFT study of oxygen reduction reaction on chromia and hematite: insights into corrosion inhibition. *J. Phys. Chem. C*, 124 (2020) 13799-13808, <https://dx.doi.org/10.1021/acs.jpcc.0c03559>.
- M. Reda, H.A. Hansen, T. Vegge. (2018). DFT study of the oxygen reduction reaction on carbon-coated iron and iron carbide. *ACS Catalysis*, DOI: 10.1021/acscatal.8b02167.
- P. Błoński, A. Kiejna, J. Hafner. (2005). Theoretical study of oxygen adsorption at the Fe (110) and (100) surfaces. *Surface Science*, 590:88–100. DOI:10.1016/j.susc.2005.06.011.
- P. Błoński, A. Kiejna, J. Hafner. (2008). Dissociative adsorption of O<sub>2</sub> molecules on O-precovered Fe (110) and Fe (100): Density functional calculations. *Physical Review B*, 77 (2008) 155424, DOI:10.1103/PhysRevB.77.155424.
- P. Giannozzi, O. Andreussi, T. Brumme, O. Bunau, M.B. Nardelli, M. Calandra, R. Car, C. Cavazzoni, D. Ceresoli, M. Cococcioni, N. Colonna, I. Carnimeo, A.D. Corso, S. de Gironcoli, P. Delugas, R. Di Stasio, A. Ferretti, A. Floris, G. Fratesi, G. Fugallo, R. Gebauer, U. Gerstmann, F. Giustino, T. Gorni, J. Jia, M. Kawamura, H.Y. Ko, A. Kokalj, E. Küçükbenli, M. Lazzeri, M. Marsili, N. Marzari, F. Mauri, N.L. Nguyen, H.V. Nguyen, A.O. de-la Roza, L. Paulatto, S. Poncé, D. Rocca, R. Sabatini, B. Santra, M. Schlipf, A.P. Seitsonen, A. Smogunov, I. Timrov, T. Thonhauser, P. Umari, N. Vast, X. Wu, S. Baroni. (2017). Advanced capabilities for materials modeling with Quantum Espresso. *J. Phys: Condens. Matter*, 29 : 465901, <https://doi.org/10.1088/1361-648X/aa8f79>.
- Rapp. (2006). An enormous breadth of engineering systems depend upon corrosion protection for their reliability, performance, and safety. *Materials Today*, 9.
- R. Kohlhaas, P. Donner, N.S. Pranghe. (1967). The temperature-dependence of the lattice parameters of iron, cobalt, and nickel in the high temperature range. *Z. Angew. Phys.*, 23 : 245.
- T.H. Fischer. (1992). General methods for geometry and wave function optimization. *J. Phys. Chem.*, 96 : 9768-9774.
- Trethewey. (1988). *Corrosion: for students of science and engineering*. Longman Scientific & Technical.
- W. Cao. (2010). Using and validation of the DFT method for oxygen adsorbed on the iron (100) surface, Mineral Processing and Extractive Metallurgy. *Trans. Inst. Min Metall. C.*, 119 (2010) 67, DOI:10.1179 / 037195510X12665949176373.
- W. Wang, G. Wang, M. Shao. (2016). First-principles modeling of direct versus oxygen-assisted water dissociation on Fe (100) surfaces. *Catalysts*. 6 (2016) 29, doi: 10.3390 / catal6020029.
- Y. Sakisaka, T. Miyano, M. Onchi. (1984). Electron-energy-loss-spectroscopy study of oxygen chemisorption and initial oxidation of Fe (100). *Physical Review B*, 30.
- Z. Chen, Y. Nonga, J. Chenb, Y. Chenb, B. Yua. (2020). A DFT study on corrosion mechanism of steel bar under water-oxygen interaction. *Computational Materials Science*, 171:109265, <https://doi.org/10.1016/j.commatsci.2019.109265>.
- Z. Chen, Y. Nonga, Y. Chenb, J. Chenb, B. Yua. (2020). Study on the adsorption of OH<sup>-</sup> and CaOH<sup>+</sup> on Fe (100) surface and their effect on passivation of steel bar: Experiments and DFT modelling. *Corrosion Science*, 174:108804, <https://doi.org/10.1016/j.corsci.2020.108804>.